Biochimica et Biophysica Acta 1860 (2016) 28–35

Contents lists available at ScienceDirect

Biochimica et Biophysica Acta

journal homepage: www.elsevier.com/locate/bbagen

CdTe quantum dots as fluorescent probes to study transferrin receptors in glioblastoma cells

Paulo E. Cabral Filho [a], Ana L.C. Cardoso [b], Maria I.A. Pereira [a], Ana P.M. Ramos [a], Fernando Hallwas [c], M. Margarida C.A. Castro [d,e], Carlos F.G.C. Geraldes [d,e], Beate S. Santos [f], Maria C. Pedroso de Lima [b], Giovannia A.L. Pereira [c], Adriana Fontes [a,*]

[a] Biophysics and Radiobiology Department, Federal University of Pernambuco, Recife, PE, Brazil
[b] CNC- Center for Neuroscience and Cell Biology, University of Coimbra, Coimbra, Portugal
[c] Department of Fundamental Chemistry, Federal University of Pernambuco, Recife, PE, Brazil
[d] Department of Life Sciences, Faculty of Science and Technology, University of Coimbra, Coimbra, Portugal
[e] Coimbra Chemistry Center, University of Coimbra, Coimbra, Portugal
[f] Department of Pharmaceutical Sciences, Federal University of Pernambuco, Recife, PE, Brazil

ARTICLE INFO

Article history:
Received 30 June 2015
Received in revised form 18 September 2015
Accepted 30 September 2015
Available online 3 October 2015

Keywords:
Nanoparticles
Cancer cells
Transferrin
Receptors
Bioconjugation
Covalent binding

ABSTRACT

Background: Overexpression of transferrin receptors (TfRs), which are responsible for the intracellular uptake of ferric transferrin (Tf), has been described in various cancers. Although molecular biology methods allow the identification of different types of receptors in cancer cells, they do not provide features about TfRs internalization, quantification and distribution on cell surface. This information can, however, be accessed by fluorescence techniques. In this work, the quantum dots (QDs)' unique properties were explored to strengthen our understanding of TfRs in cancer cells.
Methods: QDs were conjugated to Tf by covalent coupling and QDs-(Tf) bioconjugates were applied to quantify and evaluate the distribution of TfRs in two human glioblastoma cells lines, U87 and DBTRG-05MG, and also in HeLa cells by using flow cytometry and confocal microscopy.
Results: HeLa and DBTRG-05MG cells showed practically the same TfR labeling profile by QDs-(Tf), while U87 cells were less labeled by bioconjugates. Furthermore, inhibition studies demonstrated that QDs-(Tf) were able to label cells with high specificity.
Conclusions: HeLa and DBTRG-05MG cells presented a similar and a higher amount of TfR than U87 cells. Moreover, DBTRG-05MG cells are more efficient in recycling the TfR than the other two cells types.
General significance: This is the first study about TfRs in human glioblastoma cells using QDs. This new fluorescent tool can contribute to our understanding of the cancer cell biology and can help in the development of new therapies targeting these receptors.

1. Introduction

Transferrin (Tf) is a β-globin with approximately 670–700 amino acids, which binds to a cell surface receptor (TfR) expressed by most proliferating cells with particularly high expression on tumor cells, being one of the biomolecules most applied to cancer cell targeting [1]. The TfR is also known as CD71 and promotes the cellular uptake of ferric Tf [2], by clathrin-mediated endocytosis [3]. Nanotechnology approaches have taken advantage of the potential use of the TfRs to improve therapy and diagnostic procedures related to cancer. The most common systems employed for these purposes are liposomes [4,5], metallic nanoparticles [6,7] and magnetic nanoparticles [3]. These nanosystems have been functionalized with Tf to target the TfR in order to improve diagnostic methods, as well as the efficacy of chemotherapeutics, since cancer cells and tissues overexpress TfR on their surface with respect to normal cells. Zhai et al. [4], for instance, used TfRs as targets of liposomes conjugated to Tf and loaded with docetaxel, showing that these nanocarriers are a promising chemotherapeutic delivery vehicle for cancer therapeutics, when compared to liposomes lacking Tf. Therefore, studies related to the TfR can provide a better understanding of the cell biology of cancer and also help to improve its treatment.

TfRs have been widely studied by molecular biology approaches, which proved to be a valuable tool in the identification of different types of receptors in cancer cells [8–10]. However, molecular biology methods do not provide information about the cellular internalization of the receptor, its quantification and distribution. Fluorescence-based techniques have high sensitivity to quantify biomolecules with

* Corresponding author at: Av. Prof. Moraes Rego, S/N. Departamento de Biofísica e Radiobiologia, CCB, UFPE, 50670-901, Recife, PE, Brazil.
E-mail address: adriana.fontes.biofisica@gmail.com (A. Fontes).

http://dx.doi.org/10.1016/j.bbagen.2015.09.021
0304-4165/

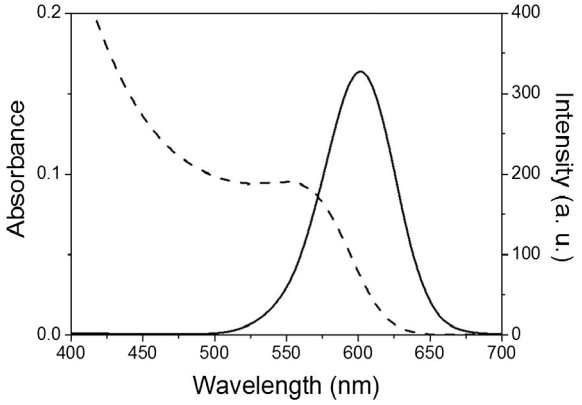

Fig. 1. Optical characterization of CdTe QDs aqueous colloidal suspension: absorption (dashed line) and emission (solid line) spectra. The excitation wavelength (λ_{exc}) for the emission spectrum was 365 nm.

high specificity and thus can be used as innovative and attractive methods to investigate receptor intracellular trafficking and distribution, complementing molecular biology studies [11]. Among the most promising probes that can be applied in fluorescence-based research are the quantum dots (QDs), which are semiconductor fluorescent nanoparticles that have great potential for biological research due to their unique optical and chemical properties. QDs present exceptional resistance to photobleaching, enabling long-term studies, and their active surface allows their functionalization with biomolecules in order to reach biological targets with a high specificity [12–15]. These QDs' features can be employed to strengthen our understanding of cellular receptors, such as the TfR.

The aim of this work was to apply CdTe QDs conjugated to Tf (QDs-Tf) as probes to study the TfRs in human glioblastoma cells, by using the complementary analyzes provided by fluorescence confocal microscopy and flow cytometry. The TfR was quantified and its distribution was analyzed in two different human glioma cells lines, U87 (glioblastoma) and DBTRG-05MG (recurrent glioblastoma). HeLa cells (human epithelial cervical carcinoma) were used as a control cellular model in this work, since QDs associated to Tf have already been applied to study the TfR in these cells [16–19]. However, the specificity of such conjugates has not been fully proved in those previous works. Here, the bioconjugation procedure of QDs to Tf was improved and the specificity of the labeling was demonstrated by TfR saturation assays. Moreover, to our knowledge, this is the first study that not

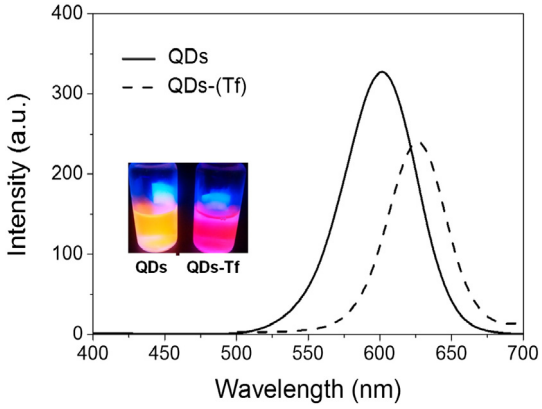

Fig. 2. Emission spectra of bare QDs (solid line) and QDs-(Tf) (dashed line). Pictures of the QDs (orange emission) and the bioconjugates (red emission) show their fluorescence under UV–Vis excitation (λ_{exc} = 365 nm).

Table 1
Fluorescence Microplate Assay results obtained from the average signal of fluorescence intensities (controls and bioconjugates) and percentage of relative fluorescence intensity of the bioconjugates.

Systems	Average of signal 4 days	RF (%) 4 days	Average of signal 10 days	RF (%) 10 days
Transferrin	151.6	–	122.6	–
QDs	212.0	–	258.0	–
QDs-(Tf)	698.0	283.9	41,615.0	21,764.0

only investigates the TfR in these two glioblastoma cell lines, but also compares the amount and the distribution of TfRs on these types of tumor cells, using the HeLa cell line as reference.

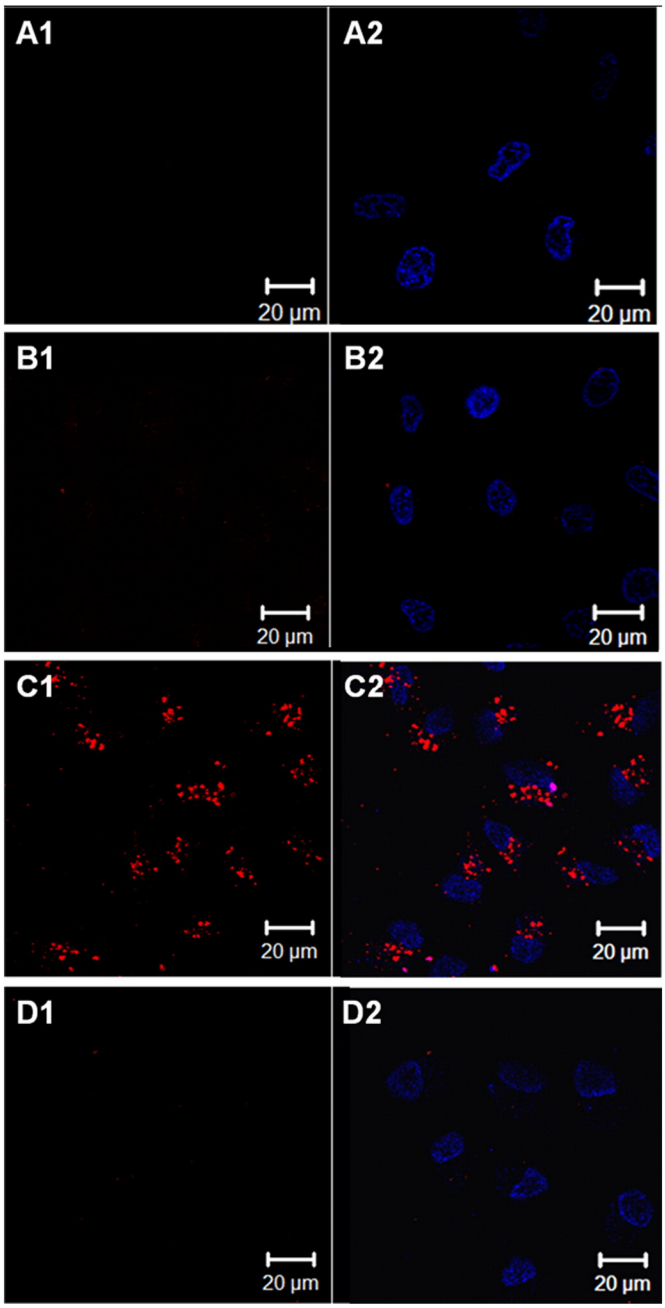

Fig. 3. Confocal microscopy images of HeLa cells labeled by QDs-(Tf). (A) Control HeLa cells, (B) HeLa cells incubated with bare QDs, (C) HeLa cells incubated with QDs-(Tf) and (D) HeLa cells incubated with QDs-(Tf) after TfR saturation. The identification (1) refers to the confocal emission channel LP 565 nm and the identification (2) refers to the overlap of LP 565 nm and Hoechst emission channel (BP 420-480 nm). Scale Bar: 20 μm.

2. Experimental procedures

2.1. Synthesis and characterization of CdTe-MSA QDs

CdTe-MSA QDs were synthesized as an aqueous colloidal dispersion according to a previously reported method, with some modifications [20]. Briefly, QDs were prepared by adding Te^{2-} ions to a $Cd(ClO_4)_2$ solution at pH > 10 in the presence of MSA (mercaptosuccinic acid) as stabilizing agent in a molar ratio of 5:1:6 (Cd:Te:MSA, respectively). The Te^{2-} aqueous solution was prepared by reducing metallic tellurium with $NaBH_4$ at a high pH and under nitrogen saturated inert atmosphere. The reaction proceeded under constant stirring and heating at 90 °C during 5 h.

After their synthesis, QDs were optically characterized by absorption and emission spectroscopy carried out on a spectrophotometer Evolution 600 UV–Vis (Thermo Scientific) and on spectrometer LS 55 (PerkinElmer, at $\lambda_{exc} = 365$ nm), respectively.

2.2. CdTe-MSA QDs conjugation to transferrin

CdTe-MSA QDs were conjugated with human holo transferrin (Tf) (Sigma Aldrich) by using N-ethyl-3-(3-dimethylaminopropyl)carbo diimide hydrochloride (EDC — Fluka) and N-hydroxysulfosuccinimide sodium salt (Sulfo-NHS — Sigma Aldrich) as coupling reagents.

First, the pH of 2 mL of the CdTe-MSA QDs dispersion (at 0.84 μM) was adjusted to 5.5 by using MSA at 4.9% (*w*/*v*). Then, 1 mL of EDC (at 4 $mg \cdot mL^{-1}$) was added and after 5 min, 1 mL of Sulfo-NHS (at 5.5 $mg \cdot mL^{-1}$) was also added to the QDs aqueous suspension [21,22]. Then, 15 min later, 194 μL of Tf (at 1 $mg \cdot mL^{-1}$) was added to reach a ratio of QDs:Tf 1:2 (particle:molecule).

Before cell labeling, the QDs-(Tf) conjugated system was incubated with 50 μL of TRIS base (at 1 mM) for 2 h under slow agitation. This procedure was used to quench the free carboxyl groups of non-conjugated QDs in order to minimize unspecific labeling. QDs-(Tf) were optically characterized by emission spectroscopy at $\lambda_{exc} = 365$ nm by using the same spectrometer mentioned above (LS 55, PerkinElmer).

2.3. Confirmation of conjugation QDs-(Tf) by Fluorescence Microplate Assay (FMA)

To confirm the efficiency of the bioconjugation process, we employed the Fluorescence Microplate Assay (FMA) [23]. Briefly, all the systems (Tf, bare QDs and QDs-(Tf)) were placed in a polystyrene microplate (black 96-well Optiplate F HB microplates — PerkinElmer) in triplicates, at the same concentration used for the bioconjugation assay. The plate was maintained for 2 h in an incubator (water bath, humid chamber) at 37 °C. After this period, the plate was washed three times with a phosphate buffered saline solution, PBS 1× (from now on named as PBS). We analyzed the conjugates as a function of time by evaluating the QDs-(Tf) samples at 4th and 10th days after the initial bioconjugation assay.

Fluorescence measurements were performed on a WALLAC 1420 Plate Reader, equipped with the software Victor^2 (PerkinElmer). The excitation band pass filter used was the BP 405 nm ± 2.5 nm and the emission band pass filter was the BP 595 nm ± 15 nm. The acquisition time was 1 s, the lamp was set to 20,000 and normal slits were used for the excitation of samples and for collecting the emission.

2.4. Cell culture

HeLa cells (human epithelial cervical carcinoma) were obtained from the American Type Culture Collection (Manassas, VA, USA) and the U87 (human glioblastoma) and DBTRG-05MG (human recurrent glioblastoma) cells were kindly provided by Dr. Peter Canoll (Columbia University, New York, NY) and Dr. Massimiliano Salerno (Siena Biotech, Italy). HeLa and U87 cells were cultured in Dulbecco's modified Eagle's medium with high glucose (DMEM — Sigma Aldrich) supplemented with 10% of fetal bovine serum (FBS — Gibco), 100 $mg \cdot mL^{-1}$ streptomycin and 100 units$\cdot mL^{-1}$ penicillin (Sigma Aldrich) at 37 °C in a humidified atmosphere with 5% CO_2. DBTRG-05MG cells were cultured in Roswell Park Memorial Institute (RPMI — Sigma Aldrich) 1640 medium supplemented with 10% of FBS, 100 $mg \cdot mL^{-1}$streptomycin and 100 units$\cdot mL^{-1}$ penicillin at 37 °C in a humidified atmosphere with 5% CO_2. When HeLa cells reached 90% confluence in the culture

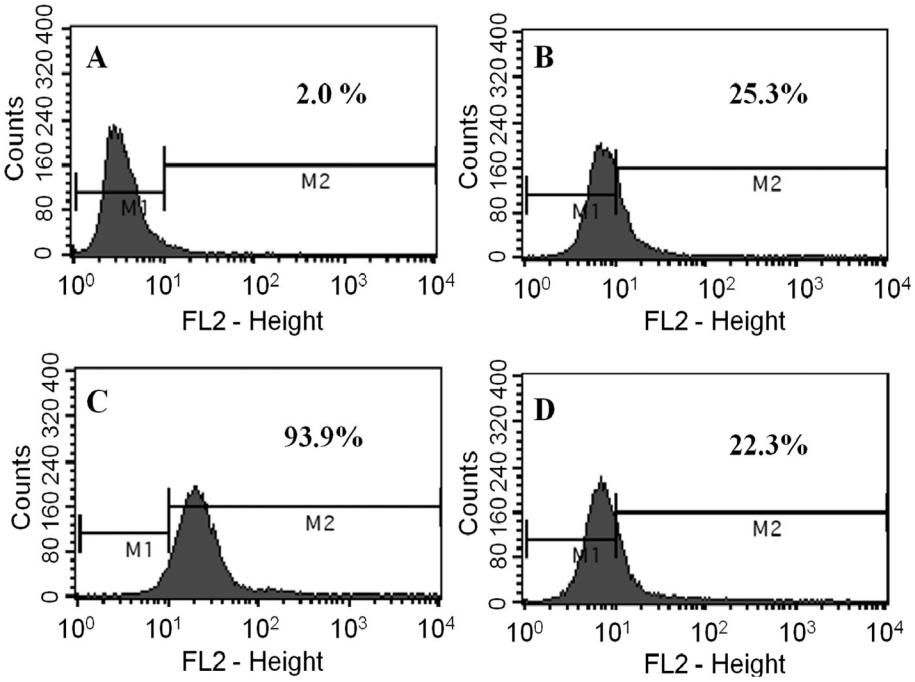

Fig. 4. Flow cytometry analysis of HeLa cells. In (A) HeLa cells in PBS, (B) HeLa cells incubated with bare QDs (C) HeLa cells incubated with QDs-(Tf) and (D) HeLa cells incubated with QDs-(Tf) after Tf-receptor saturation.

flask, they were detached with 0.25% of trypsin (Sigma Aldrich) in Dissociation Buffer (Gibco). Detachment of U87 and DBTRG cells was performed exclusively with Dissociation Buffer. The cells were then seeded onto a 6-well plate (1.5 x 10^5 cells/well — Thermo Scientific™ BioLite) and incubated for 24 h for flow cytometry studies and in an 8-well plate (2.0 × 10^4 cells/well — μSlide IbiTreat, Germany) for confocal microscopy analysis. At this time point, cells exhibited a confluence of around 80–90% in the wells.

2.5. Labeling cancer cells with QDs-(Tf)

After incubation for 24 h in 6-well or 8-well plates, the cells were washed with PBS and the following experimental conditions were assayed: (I) control cells with PBS; (II) PBS and bare QDs (1:1 *v*/*v*); (III) PBS and QDs-(Tf) (1:1 *v*/*v*). After 1 h of incubation at 37 °C, the cells were washed with PBS before flow cytometry and confocal microscopy analysis to remove any residual labeling on the cell surface by bare QDs.

The percentage of labeled cells was determined by flow cytometry (FACSCalibur™, Becton Dickinson). In these studies, HeLa cells were detached from the 6-well plate upon incubation with trypsin 0.25% in Dissociation Buffer followed by trypsin inactivation with DMEM and then placed in suspension. U87 and DBTRG cells were detached exclusively with Dissociation Buffer. The cell suspensions were washed 3 times with PBS and pelleted by centrifugation at 1200 × *g*, 30 s (MiniSpin — Eppendorf). Around 20,000 events were acquired for each experimental condition following excitation at 488 nm. The emission was detected with the band pass filter 585/20 nm and the collected data were processed by the Cell Pro Software (Cell Quest™, Becton-Dickinson).

For confocal analysis, and following the establishment of different experimental conditions, the cells plated onto 8-well plates were washed three times with PBS. The cell nuclei were stained for 5 min with the fluorescent DNA-binding dye Hoechst 33,342 (at a final concentration of 1 $\mu g \cdot mL^{-1}$), and the cells were washed with PBS three times before being observed under a confocal microscope (Zeiss LSM 510 META).

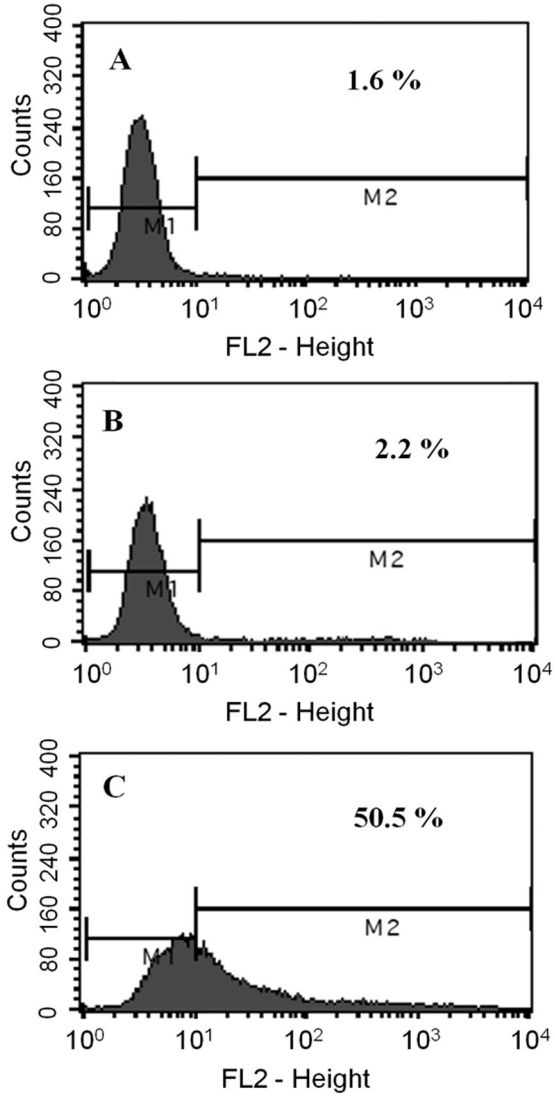

Fig. 5. Flow cytometry analysis of HeLa cells following incubation at 4 °C. (A) HeLa cells in PBS, (B) HeLa cells incubated with bare QDs, and (C) HeLa cells incubated with QDs-(Tf).

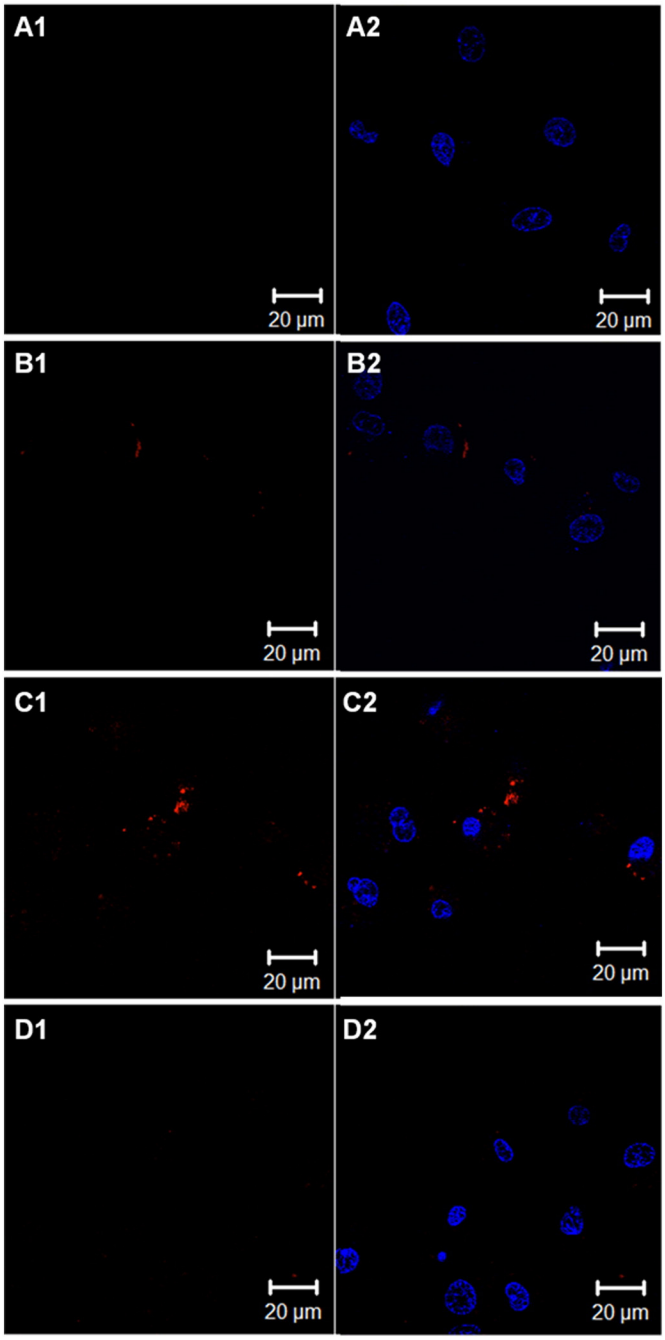

Fig. 6. Confocal microscopy images of U87 cells labeled by QDs-(Tf). (A) Control U87 cells, (B) U87 cells incubated with bare QDs, (C) U87 cells incubated with QDs-(Tf) and (D) U87 cells incubated with QDs-(Tf) after TfR saturation. The identification (1) refers to the confocal emission channel LP 565 nm and the identification (2) refers to the overlap of LP 565 nm and Hoechst emission channel (BP 420-480 nm). Scale Bar: 20 μm.

In order to confirm the specificity of the labeling, as well as the efficiency of the bioconjugation, cells were also incubated with excess of free human holo transferrin (at a final concentration of 10 mg·mL^{-1}) for 1 h at 37 °C, aiming at saturating the TFRs [24], before the confocal analysis. After this period, the cells were incubated with QDs-(Tf) for 1 additional hour at a final QDs-(Tf): free Tf ratio of 1:1 (*v*/*v*).

3. Results and discussion

3.1. Characterization of CdTe QDs and bioconjugates

According to optical characterizations, MSA QDs aqueous suspension presented a first maximum absorption peak at 548 nm, as can be observed in Fig. 1. By using the Dagtepe et al. [25] equation and the Rogach et al. [26] approximation, we estimated an average diameter of approximately 3.1 nm for these nanoparticles. Furthermore, taking into account the absorbance at the first maximum absorption peak, the CdTe QDs molar extinction coefficient proposed by Yu et al., [27] and the Lambert-Beer equation, we also estimated the QDs concentration as approximately 4.8 μM. The QDs colloidal suspension showed an emission maximum at 602 nm and a full width at a half maximum (FWHM) of about 58 nm, indicating a narrow emission spectrum (Fig. 1) which is ascribed to the exciton recombination.

Bare QDs and QDs-(Tf) (bioconjugates) exhibited similar emission spectra profiles for emission spectra (Fig. 2, $\lambda_{exc} = 365$ nm), however QDs-(Tf) showed a maximum emission at 626 nm. The observed red shift for the QDs-(Tf) suggests modifications on the QDs surface due to the bioconjugation process. The same behavior was observed in previous works using hydrophilic QDs conjugated to Concanavalin A [28] and to *Ulex europaeus* lectins [29]. In both cases the red shift of the emission peak was observed. Despite the red shift, QDs bioconjugates suspension remained highly fluorescent, as shown in Fig. 2.

3.2. Fluorescence Microplate Assay

The *FMA* results are presented in Table 1 as the average of the fluorescent signal of triplicate wells for controls and conjugates. The data analysis was carried out according to Carvalho et al. [23]. The relative fluorescence (RF) results for QDs-(Tf) were 283.9% and 21,764.0%, for the 4th and 10th days after bioconjugation, respectively. According to Carvalho et al. [23] the bioconjugation process is efficient when the bioconjugates show a RF higher than 100%. Therefore, our results (Table 1) indicate that the bioconjugation was efficient after four days and improved over time. The Sigma Aldrich product information indicates that Tf should remain active at 4 °C for 5–10 days after dilution.

3.3. Labeling HeLa cells by using QDs-(Tf)

As shown in Fig. 3, efficient and specific labeling of the TfR was observed in HeLa cells using QDs-(Tf) (Fig. 3, C1 and C2). HeLa cells, incubated with bare QDs (Fig. 3, B1 and B2), as well as after TfR saturation by free Tf (Fig. 3, D1 and D2), did not show considerable labeling, resulting in an image profile similar to the one obtained for control (in the absence of QDs) HeLa cells (Fig. 3, A1 and A2). The use of the DNA-binding dye Hoechst allowed to detect the intracellular localization of the receptor, indicating that 1 h of cell incubation with the QDs-(Tf) was sufficient to promote the internalization of the TfR by HeLa cells.

The confocal microscopy results were confirmed by flow cytometry analysis. As shown in Fig. 4C, about 94% of HeLa cells were labeled by QDs-(Tf), while incubation of the cells with bare QDs (Fig. 4B) or after inhibiting the specific interaction of QDs-(Tf) with TfRs (Fig. 4D), resulted in less than 26% of cell labeling. The residual labeling, less than 26%, may be attributed to QDs internalization by a TfR-independent pathway. This type of unspecific interaction between the cells and nanoparticles has been previously reported [30–32].

These results were confirmed by incubating the cells at 4 °C (Fig. 5), under which conditions endocytosis is compromised [33]. As shown in Fig. 5B, HeLa cells labeling by bare QDs was inhibited. On the other hand, QDs-(Tf) labeled 50.5% of HeLa cells (Fig. 5C) corresponding to the labeling of TfRs that remained on the cell surface, since the receptors cannot be internalized at this temperature, resulting in a decrease of labeled cells of approximately 43%, when compared to what was observed at 37 °C (Fig. 4C). Therefore, our results demonstrated specific

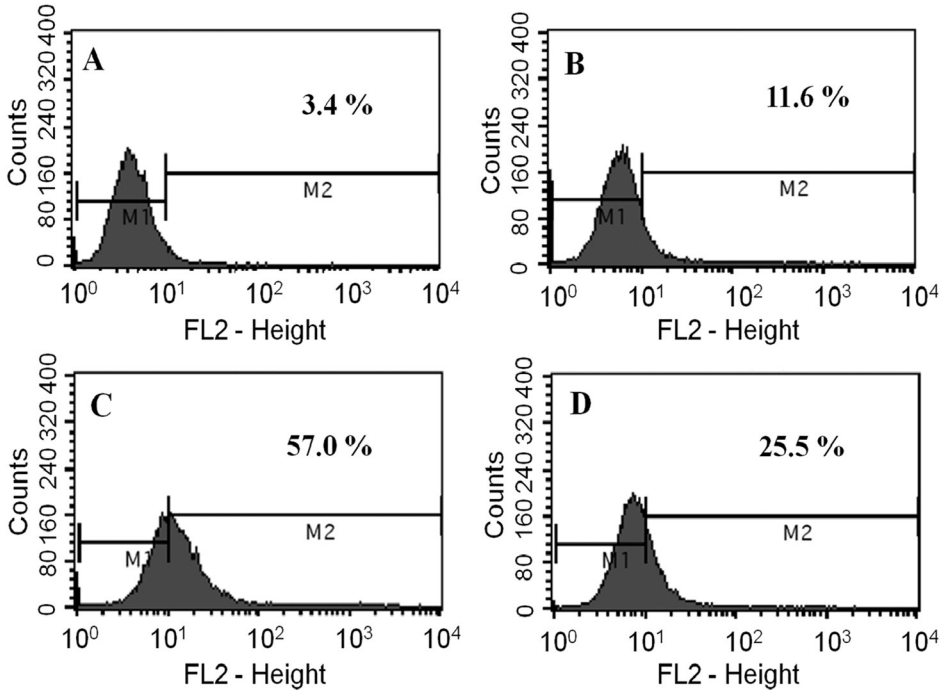

Fig. 7. Flow cytometry analysis of U87 cells. (A) U87 cells in PBS, (B) U87 cells incubated with bare QDs (C) U87 cells incubated with QDs-(Tf) and (D) U87 cells incubated with QDs-(Tf) after TfR saturation.

interaction of QDs- (Tf) with TfRs, which promoted cellular internalization of the QDs-(Tf).

In this work, HeLa cells were used as a model cell system and experimental approaches involving the blocking of TfR or inhibition of TfR-mediated endocytosis were employed to confirm the efficiency and specificity of QDs-(Tf) conjugates. Indeed, although the TfR has been studied by fluorescence assays with QDs [16,18,34,35], the targeting specificity of such conjugates has not been fully demonstrated. Sahoo et al. used polymeric nanoparticles (NPs) conjugated to Tf and showed that when NPs-Tf were incubated with an excess of Tf (50 μg), the percentage of labeled MCF-7 cells (a breast cancer cell line) was similar to that obtained when the cells were incubated with bare NPs [36]. These results are in agreement with our findings showing the specificity of the TfR labeling by QDs-Tf in HeLa cells. In this regard, less than 23% of HeLa cells were labeled after TfR saturation (Fig. 4D), this labeling being most likely attributed to QDs-(Tf) non-specific endocytosis, consistent with the results observed when HeLa cells were incubated with bare QDs, which do not exhibit affinity to TfR (Fig. 4B). To our knowledge, this is the first study addressing TfR saturation through competitive inhibition experiments with free Tf to confirm that the cell internalization of QDs-(Tf) bioconjugates is specific for TfRs.

Our results showed that 1 h of incubation with QDs-(Tf) was sufficient to promote their internalization through specific interaction with TfRs in HeLa cells. These achievements agree with those presented by Chan et al. and Tekle et al. that applied QDs-(Tf) to label specifically the TfR in HeLa cells [16,19]. Guan et al. carried out three different types of conjugations by using QDs and Tf, and showed that the most efficient was the one using EDC as coupling agent [18]. The authors demonstrated that approximately 85.5% of cells were labeled by QDs-Tf. Our results using EDC and Sulfo-NHS presented an improvement relative to these previous studies, showing a labeling percentage of about 93%. To our best knowledge, this is the first work that used EDC and Sulfo-NHS simultaneously as coupling agents to conjugate MSA-QDs to Tf. According to Hermanson [22], the simultaneous use of these coupling agents improves the bioconjugation process by minimizing the generation of reactive species, when compared to the individual use of EDC for bioconjugation purposes.

3.4. Labeling glioblastoma cells by using QDs-(Tf)

In studies addressing the TfR in glioblastoma cells, we employed the U87 human glioblastoma cell line, extensively reported as a relevant glioblastoma cellular model and the DBTRG-05MG cell line, established from a glioblastoma patient treated with local brain irradiation and multidrug chemotherapy. Confocal microscopy images of U87 cells, displayed in Fig. 6, show that the TfR is present in a minimal amount, since a very small amount of labeling could be observed following incubation with QDs-(Tf) (Fig. 6, C1 and C2). Blocking Tf-receptor by adding excess of free Tf decreased even further the cell labeling (Fig. 6, D1 and D2), and similar results were obtained after cell incubation with bare QDs (Fig. 6, B1 and B2).

The confocal microscopy results were confirmed by quantitative flow cytometry analysis of U87 cells, as illustrated in Fig. 7. Fig. 7C shows that 57.0% of U87 cells were labeled when incubated with QDs-(Tf). On the other hand, only 25.5% of cells were labeled after TfR saturation (Fig. 7D).

According to Dixit et al. [7], when U87 cells were incubated with gold nanoparticles functionalized by the Tf peptide, an accumulation of these nanostructures was observed inside the cells after 1 h, which increased until 24 h. The results of that study indicated that the endocytic activity of U87 cells occurs at a slower rate when compared to that of LN299 cells, another human glioma cell line, with an uptake plateau after 1 h. In agreement with the findings reported by Dixit et al., our results showed that U87 cells internalize QDs-(Tf) at a low extent which also seem to have a small amount of TfRs at the plasma membrane.

In contrast with U87 cells, confocal microscopy images of DBTRG-05MG cells incubated with QDs-(Tf) (Fig. 8, C1 and C2) showed that TfR internalization was very effective in these cells. After 1 h incubation with QDs-(Tf), DBTRG-05MG cells showed a similar profile to that in HeLa cells, regarding the presence of the TfR (Fig. 8C and Fig. 3C, respectively). Furthermore, when DBTRG-05MG cells were incubated with bare QDs (Fig. 8, B1 and B2) no significant unspecific labeling was observed. However, when these cells were incubated with QDs-(Tf), after TfR saturation with free Tf (Fig. 8, D1 and D2), fluorescent labeling in some cells was detected.

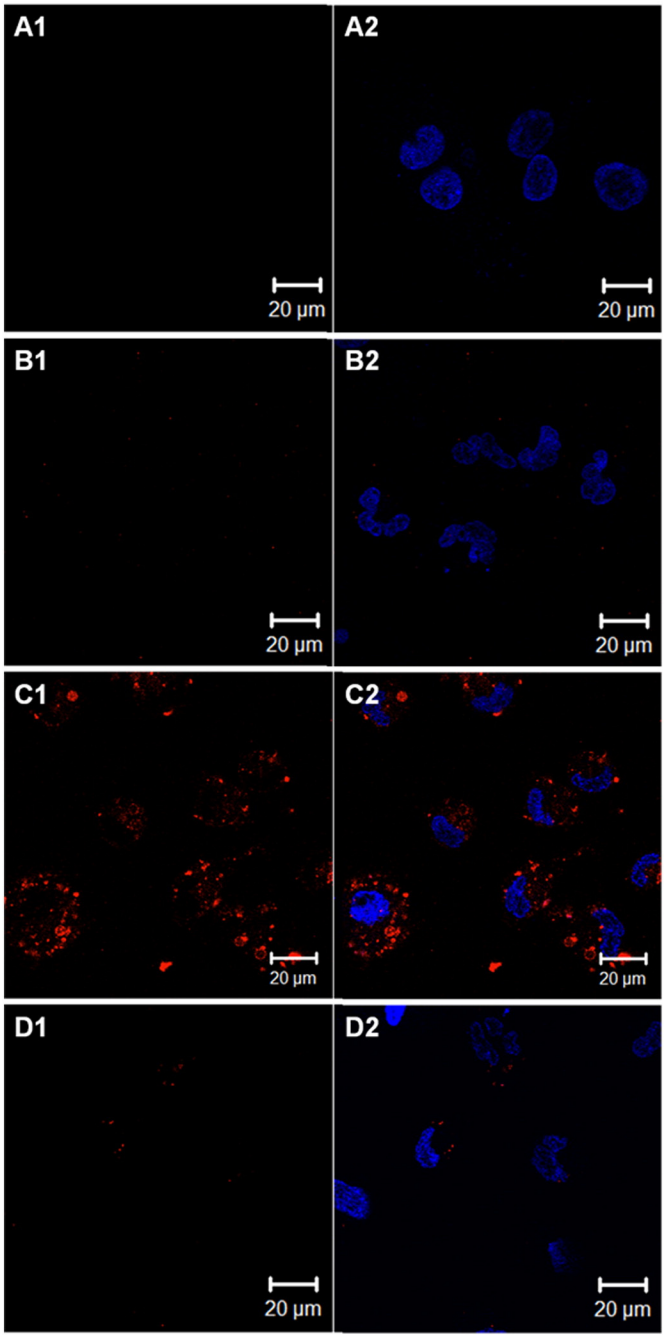

Fig. 8. Confocal microscopy images of DBTRG-05MG cells labeled by QDs-(Tf). (A) Control DBTRG-05MG cells (B) DBTRG-05MG cells incubated with bare QDs, (C) DBTRG-05MG cells incubated with QDs-(Tf) and (D) DBTRG-05MG cells incubated with QDs-(Tf) after TfR saturation. The identification (1) refers to the confocal emission channel LP 565 nm and the identification (2) refers to the overlap of LP 565 nm and Hoechst emission channel (BP 420-480 nm). Scale Bar: 20 μm.

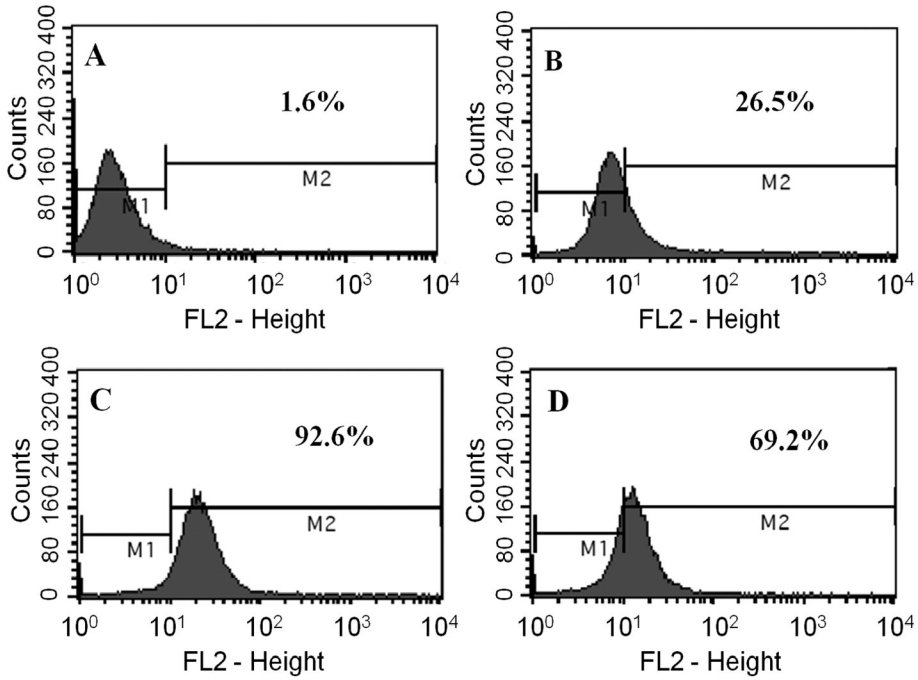

Fig. 9. Flow cytometry analysis in DBTRG-05MG cells. (A) DBTRG-05MG cells in PBS, (B) DBTRG-05MG cells incubated with bare QDs, (C) DBTRG-05MG cells incubated with QDs-(Tf) and (D) DBTRG-05MG cells incubated with QDs-(Tf) after TfR saturation.

These results obtained by confocal microscopy were confirmed through flow cytometry analysis (Fig. 9). Approximately 93% of DBTRG-05MG cells were positively labeled after 1 h incubation with QDs-(Tf) (Fig. 9C), indicating that these cells express a high amount of TfRs. However, when the cells were incubated with bare QDs, a significant decrease in the percentage of labeled cells was observed to about 26% (Fig. 9B). Furthermore, when the TfR was blocked by addition of excess free Tf, 69.2% of DBTRG-05MG cells still presented labeling by QDs-(Tf) (Fig. 9D), corroborating the observations made by confocal microscopy. Taken together, these results denote a more efficient TfR recycling in these cells as compared to U87 or HeLa cells, which can be attributed to a higher metabolic activity of DBTRG-05MG cells [37].

As mentioned before, the DBTRG-05MG cell line was originated from the tumor tissue of a patient owing a recurrent glioblastoma that has been treated with irradiation and chemotherapy [38]. This variant of glioblastoma is more aggressive and resistant to current chemotherapy when compared to that originated from U87 cells [39–41], which can also justify the high metabolic rate and the probably faster recycling of the TfR observed in DBTRG-05MG cells.

Moreover, our results demonstrate that HeLa and DBTRG-05MG cells express and internalize comparable amounts of TfRs, showing 94% and 93% of cells labeled by QDs-(Tf), respectively, while U87 cells present a lower quantity of TfRs, associated to a lower extent of internalization of these receptors, resulting in 57% of cells labeled by QDs-(Tf).

Fig. 10 shows comparative confocal microscopy images of the three cell lines, HeLa (Fig. 10A), U87 (Fig. 10B) and DBTRG-05MG (Fig. 10C), after incubation with QDs-(Tf). As observed, after 1 h of incubation, TfRs are accumulated inside HeLa and DBTRG-05MG cells in endocytic vesicles, indicating an efficient uptake of these receptors. This kind of internalization profile has already been reported previously in HeLa cells [16,19,35]. On the other hand, U87 cells (Fig. 10B) present a lower amount of TfRs, and the conjugates seem to be preferentially located at the cell membrane level, suggesting a lower endocytosis extent when compared to HeLa or DBTRG-05MG cells.

4. Conclusions

QDs-(Tf) were used in this work to quantify the expression and study the traffic of the TfRs in different types of mammalian cancer cells. HeLa and DBTRG-05MG cells present a similar amount of TfR, while U87 cells demonstrated to have a lower quantity of this receptor, when compared to the other two cell lines. Furthermore, DBTRG-05MG cells were more efficient in promoting the recycling of TfRs than HeLa or U87 cells. Therefore, this work suggests that a specific chemotherapeutic drug delivery

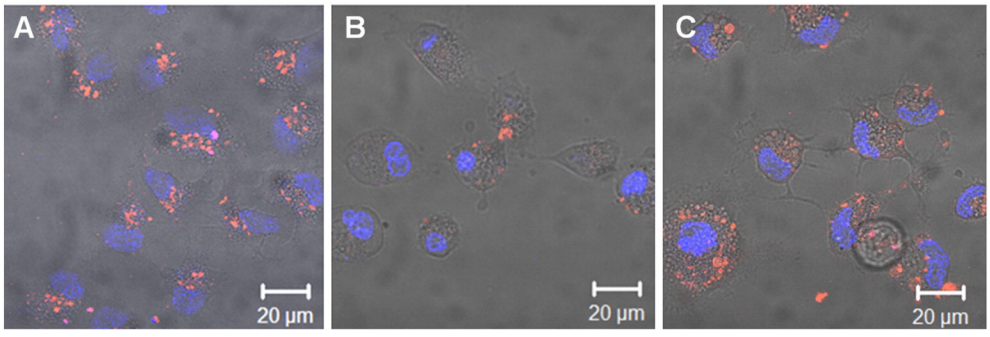

Fig. 10. Confocal microscopy images comparing HeLa, U87 and DBTRG-05MG cells following labeling by QDs-(Tf). These micrographs are overlaps of the confocal filters: LP 565, BP 420–480 nm emission and DIC. (A) HeLa cells, (B) U87 cells and (C) DBTRG-05MG cells. Scale bar: 20 nm.

system targeting TfRs could be more effective in DBTRG-05MG and HeLa cancer cells than in U87. This is an interesting result, particularly taking into consideration the fact that DBTRG-05MG cells are originated from a recurrent glioblastoma, while U87 cells derive from a primary tumor, which suggests that TfRs may play an important role in cancer cell maintenance in recurrent situations.

Overall, the results presented in this study illustrate that QDs-(Tf) can be applied to quantify TfR expression and also to study the dynamics of this receptor in different types of cancer cells. Therefore, we believe that this biophotonic tool can be of great value in future studies in cancer cell biology. The understanding of the molecular aspects of cancer cell biology can help to develop new and effective therapies for this disease, such as those targeting TfRs as a specific and efficient entry pathway for chemotherapeutic drugs.

Author contributions

PECF participated in all experiments involved in the study; MIAP and APMR synthesized and characterized the QDs and conjugates; GALP, MMC and FH analyzed and discussed the bioconjugation; ALC, MCPL, PECF and AF interpreted the microscopy and flow cytometry results; AF, BSS, GALP and CFGCG conceived and designed the experiments. All authors read and approved the final manuscript.

Disclosure

The authors confirm that there are no conflicts of interest in this work.

Acknowledgments

This work was supported by the Brazilian agencies: the Coordination for the Improvement of Higher Education Personnel (CAPES), through the Transnational Cooperation Program CAPES/FCT (331/13), the National Council for Scientific and Technological Development (CNPq), and the Foundation for Science and Technology of Pernambuco (FACEPE). This work is also linked to the National Institute of Photonics (INFo).

Transparency document

The Transparency document associated with this article can be found in the online version.

References

[1] H. Li, Z.M. Qian, Transferrin/transferrin receptor-mediated drug delivery, Med. Res. Rev. 22 (2002) 225–250.
[2] T.R. Daniels, E. Bernabeu, J.A. Rodríguez, S. Patel, M. Kozman, D.A. Chiappetta, E. Holler, J.Y. Ljubimova, G. Helguera, M.L. Penichet, Transferrin receptors and the targeted delivery of therapeutic agents against cancer, Biochim. Biophys. Acta 1820 (2012) 291–317.
[3] W. Ding, L. Guo, Immobilized transferrin Fe(3)O(4)@SiO(2) nanoparticle with high doxorubicin loading for dual-targeted tumor drug delivery, Int. J. Nanomedicine 8 (2013) 4631–4639.
[4] G. Zhai, J. Wu, B. Yu, C. Guo, X. Yang, R.J. Lee, A transferrin receptor-targeted liposomal formulation for docetaxel, J. Nanosci. Nanotechnol. 10 (2010) 5129–5136.
[5] H. Li, H. Sun, Z.M. Qian, The role of the transferrin–transferrin-receptor system in drug delivery and targeting, Trends Pharmacol. Sci. 23 (2002) 206–209.
[6] D.T. Wiley, P. Webster, A. Gale, M.E. Davis, Transcytosis and brain uptake of transferrin-containing nanoparticles by tuning avidity to transferrin receptor, Proc. Natl. Acad. Sci. U. S. A. 110 (2013) 8662–8667.
[7] S. Dixit, T. Novak, K. Miller, Y. Zhu, M.E. Kenney, A.-M. Broome, Transferrin receptor-targeted theranostic gold nanoparticles for photosensitizer delivery in brain tumors, Nanoscale 7 (2015) 1782–1790.
[8] D.J. Yoon, D.S.H. Chu, C.W. Ng, E.A. Pham, A.B. Mason, D. Hudson, V.C. Smith, R.T.A. MacGillivray, D.T. Kamei, Genetically engineering transferrin to improve its in vitro ability to deliver cytotoxins, J. Control. Release 133 (2009) 178–184.
[9] P. Ponka, C.N. Lok, The transferrin receptor: role in health and disease, Int. J. Biochem. Cell Biol. 31 (1999) 1111–1137.
[10] E.W. Müllner, L.C. Kühn, A stem-loop in the 3′ untranslated region mediates iron-dependent regulation of transferrin receptor mRNA stability in the cytoplasm, Cell 53 (1988) 815–825.
[11] L. Jing, K. Ding, S.V. Kershaw, I.M. Kempson, A.L. Rogach, M. Gao, Magnetically engineered semiconductor quantum dots as multimodal imaging probes, Adv. Mater. 26 (2014) 6367–6386.
[12] A. Sukhanova, I. Nabiev, Fluorescent nanocrystal quantum dots as medical diagnostic tools, Expert Opinion on Medical Diagnostics, 2 2008, pp. 429–447.
[13] I.L. Medintz, H.T. Uyeda, E.R. Goldman, H. Mattoussi, Quantum dot bioconjugates for imaging, labelling and sensing, Nat. Mater. 4 (2005) 435–446.
[14] X. Michalet, F.F. Pinaud, L.A. Bentolila, J.M. Tsay, S. Doose, J.J. Li, G. Sundaresan, A.M. Wu, S.S. Gambhir, S. Weiss, Quantum dots for live cells, in vivo imaging, and diagnostics, Science 307 (2005) 538–544.
[15] P. Alivisatos, The use of nanocrystals in biological detection, Nat. Biotechnol. 22 (2004) 47–52.
[16] W.C.W. Chan, S. Nie, Quantum dot bioconjugates for ultrasensitive nonisotopic detection, Science 281 (1998) 2016–2018.
[17] C. Schieber, A. Bestetti, J.P. Lim, A.D. Ryan, T.-L. Nguyen, R. Eldridge, A.R. White, P.A. Gleeson, P.S. Donnelly, S.J. Williams, P. Mulvaney, Conjugation of transferrin to azide-modified CdSe/ZnS core–shell quantum dots using cyclooctyne click chemistry, Angew. Chem. Int. Ed. 51 (2012) 10523–10527.
[18] L.-Y. Guan, Y.-Q. Li, S. Lin, M.-Z. Zhang, J. Chen, Z.-Y. Ma, Y.-D. Zhao, Characterization of CdTe/CdSe quantum dots-transferrin fluorescent probes for cellular labeling, Anal. Chim. Acta 741 (2012) 86–92.
[19] C. Tekle, B.v. Deurs, K. Sandvig, T.-G. Iversen, Cellular trafficking of quantum dot-ligand bioconjugates and their induction of changes in normal routing of unconjugated ligands, Nano Lett. 8 (2008) 1858–1865.
[20] C.G. Andrade, P.E. Cabral Filho, D.P.L. Tenório, B.S. Santos, E.I.C. Beltrão, A. Fontes, L.B. Carvalho, Evaluation of glycophenotype in breast cancer by quantum dot-lectin histochemistry, Int. J. Nanomedicine 8 (2013) 4623–4629.
[21] J. Wang, X. Huang, F. Zan, C.-g. Guo, C. Cao, J. Ren, Studies on bioconjugation of quantum dots using capillary electrophoresis and fluorescence correlation spectroscopy, Electrophoresis 33 (2012) 1987–1995.
[22] G.T. Hermanson, Chapter 3 — zero-length crosslinkers, in: G.T. Hermanson (Ed.), Bioconjugate Techniques, second editionAcademic Press, New York 2008, pp. 213–233.
[23] K.H.G. Carvalho, A.G. Brasi, P.E.C. Filho, D.P.L.A. Tenorio, A.C.A. de Siqueira, E.S. Leite, A. Fontes, B.S. Santos, Fluorescence plate reader for quantum dot-protein bioconjugation analysis, J. Nanosci. Nanotechnol. 14 (2014) 3320–3327.
[24] A.L.C. Cardoso, S. Simões, L.P. de Almeida, N. Plesnila, M.C. Pedroso de Lima, E. Wagner, C. Culmsee, Tf-lipoplexes for neuronal siRNA delivery: a promising system to mediate gene silencing in the CNS, J. Control. Release 132 (2008) 113–123.
[25] P. Dagtepe, V. Chikan, J. Jasinski, V.J. Leppert, Quantized growth of CdTe quantum dots; observation of magic-sized CdTe quantum dots, J. Phys. Chem. C 111 (2007) 14977–14983.
[26] A.L. Rogach, T. Franzl, T.A. Klar, J. Feldmann, N. Gaponik, V. Lesnyak, A. Shavel, A. Eychmüller, Y.P. Rakovich, J.F. Donegan, Aqueous synthesis of thiol-capped CdTe nanocrystals: state-of-the-art, J. Phys. Chem. C 111 (2007) 14628–14637.
[27] W.W. Yu, L. Qu, W. Guo, X. Peng, Experimental determination of the extinction coefficient of CdTe, CdSe, and CdS nanocrystals, Chem. Mater. 15 (2003) 2854–2860.
[28] J.-H. Wang, Y.-Q. Li, H.-L. Zhang, H.-Q. Wang, S. Lin, J. Chen, Y.-D. Zhao, Q.-M. Luo, Bioconjugation of concanavalin and CdTe quantum dots and the detection of glucose, Colloids Surf. A Physicochem. Eng. Asp. 364 (2010) 82–86.
[29] P.E. Cabral Filho, M.I.A. Pereira, H.P. Fernandes, A.A. de Thomaz, C.L. Cesar, B.S. Santos, M.L. Barjas-Castro, A. Fontes, Blood groups antigens studies using CdTe quantum dots and flow cytometry, Int. J. Nanomedicine 10 (2015) 4393–4404.
[30] S. Zhang, J. Li, G. Lykotrafitis, G. Bao, S. Suresh, Size-Dependent Endocytosis of Nanoparticles, Advanced materials (Deerfield Beach, Fla.), 21 2009, pp. 419–424.
[31] K.-T. Yong, H. Ding, I. Roy, W.-C. Law, E.J. Bergey, A. Maitra, P.N. Prasad, Imaging pancreatic cancer using bioconjugated InP quantum dots, ACS Nano 3 (2009) 502–510.
[32] D. Chen, G. Xu, B.A. Ali, K.-T. Yong, C. Zhou, X. Wang, J. Qu, P.N. Prasad, H. Niu, Uptake of transferrin-conjugated quantum dots in single living cells, Chin. Opt. Lett. 8 (2010) 940–943.
[33] V. Biju, T. Itoh, M. Ishikawa, Delivering quantum dots to cells: bioconjugated quantum dots for targeted and nonspecific extracellular and intracellular imaging, Chem. Soc. Rev. 39 (2010) 3031–3056.
[34] P.R. Sager, P.A. Brown, R.D. Berlin, Analysis of transferrin recycling in mitotic and interphase hela cells by quantitative fluorescence microscopy, Cell 39 (1984) 275–282.
[35] M.-Z. Zhang, R.-N. Yu, J. Chen, Z.-Y. Ma, Y.-D. Zhao, Targeted quantum dots fluorescence probes functionalized with aptamer and peptide for transferrin receptor on tumor cells, Nanotechnology 23 (2012) 485104.
[36] S.K. Sahoo, V. Labhasetwar, Enhanced antiproliferative activity of transferrin-conjugated paclitaxel-loaded nanoparticles is mediated via sustained intracellular drug retention, Mol. Pharm. 2 (2005) 373–383.
[37] N.-M. Tsai, S.-Z. Lin, C.-C. Lee, S.-P. Chen, H.-C. Su, W.-L. Chang, H.-J. Harn, The antitumor effects of angelica sinensis on malignant brain tumors in vitro and in vivo, Clin. Cancer Res. 11 (2005) 3475–3484.
[38] C.A. Kruse, D.H. Mitchell, B.K. Kleinschmidt-DeMasters, W.A. Franklin, H.G. Morse, E.B. Spector, K.O. Lillehei, Characterization of a continuous human glioma cell line DBTRG-05MG: growth kinetics, karyotype, receptor expression, and tumor suppressor gene analyses, In Vitro Cell. Dev. Biol. Anim. 28 (1992) 609–614.
[39] M.M. Zulkifli, R. Ibrahim, A.M. Ali, I. Aini, H. Jaafar, S.S. Hilda, N.B. Alitheen, J.M. Abdullah, Newcastle diseases virus strain V4UPM displayed oncolytic ability against experimental human malignant glioma, Neurol. Res. 31 (2009) 3–10.
[40] P.-C. Lin, T.-W. Chiou, H.-J. Harn, An evidence-based perspective of Angelica Sinensis (Chinese Angelica) for cancer patients, in: W.C.S. Cho (Ed.), Evidence-based Anticancer Materia Medica, Springer, Netherlands 2011, pp. 131–153.
[41] R. Wondergem, J.W. Bartley, Menthol increases human glioblastoma intracellular Ca(2+), BK channel activity and cell migration, J. Biomed. Sci. 16 (2009) 90-90.